FINITE ELEMENT IMPLEMENTATION OF INTRINSIC FIELD TENSORS: AN EXAMINATION OF FREE-EDGE SINGULARITIES IN COMPOSITE LAMINATES

Daniel J. O'Shea[1], David C. Kellermann[2] and Mario M. Attard[3]

[1] School of Civil and Environmental Engineering, UNSW Australia
d.oshea@unsw.edu.au
[2] School of Mechanical and Manufacturing Engineering, UNSW Australia
d.kellermann@unsw.edu.au
[3] School of Civil and Environmental Engineering, UNSW Australia
m.attard@unsw.edu.au

Keywords: continuum mechanics, finite element, free-edge singularity, asymmetric strain tensor

ABSTRACT

This paper presents the implementation of a novel orthotropic-based elasticity theory into finite element applications; employing it to the analysis of interlaminar stress behaviour of multi-layered fibre-reinforced composites. At the scale of infinitesimal deformations, classical continuum mechanics enforces an equilibrium condition based on the geometric deformations of the body (assuming an averaging of shear strains), thus utilises symmetric linearized strain and stress tensors. The new approach imparted here resolves material rotations and equilibrium as a function of the intrinsic material properties of the continuum in addition to geometric deformations; replacing the classical strain tensor with an orthotropic-based *Intrinsic Field Tensor*. This has significant advantages when modelling strongly orthotropic media, generating an asymmetric linear strain tensor capable of describing the intricate directional nature and response of the continuum. In this paper, a novel eight-node linear hexahedral finite element is derived, capturing the new elasticity theory through the incorporation of rotational degrees of freedom and a modified constitutive law. The effects of the new theory on studying interlaminar behaviour of fibre-reinforced composites are readily apparent when observing the well-researched and longstanding free-edge stress singularity problem, and comparing to the classical mechanical approach.

1 INTRODUCTION

Substantial deficiencies remain in accurately determining the stress field in multi-layered composites due to their orthotropic nature; limiting predictive capabilities in engineering analysis. Classical methods of modelling transversely isotropic structures, such as a fibre-reinforced laminate, give rise to non-physical stresses at the intersection of an interface plane between any two dissimilar layers and the free-edge. This is commonly referred to as the free-edge singularity problem in composite laminates[1-4]. Notably, this is a typical site where delamination initiates, and we are therefore currently restricted in predictions of this critical failure mode[5]. This paper aims to assess the influence that opposing anisotropic principle material directions in adjacent bonded plies has on the development of these singularities. A novel approach is presented which applies an orthotropic elasticity theory, based on *Intrinsic-Field Tensors* (IFTs), to conventional finite element methods. This improves the modelling of complex directional-behaviour and deformation modes, in addition to describing the impact of micropolar couplings that occur in laminated fibre-reinforced composites. This is achieved by incorporating additional rotational degrees of freedom to finite element analyses –

though not requiring a length scale as in Cosserat theory[6] – which allows us to capture novel asymmetric linear strain and stress tensors. These asymmetries are driven by the micropolar coupling that occurs between adjacent directional layers of the laminate. The new orthotropic elastic constitutive law presented by Kellermann[7] is introduced to conventional finite element methods such that equilibrium is maintained on both an elemental and global level – significantly without any additional constraints or special treatment at the interface required. Preliminary results show a distinct difference in stress predictions at the intersection of the interface plane between layers and the free-edge in composite laminates under uniaxial tension, in comparison to classical mechanical techniques.

In classical mechanics, equilibrium is enforced as a result of an imposed strain symmetry condition. The new approach removes the requisite assumption of symmetry – instead equilibrium is now resolved on both an elemental and global level as a function of the intrinsic material properties of the system itself. In a composite laminate, two adjacent layers of dissimilar orthotropic material will possess distinct asymmetric strain tensors as a result of the unique directional response of each. The IFT approach allows for this to occur, whilst also maintaining compatibility of the strain field across the ply interface without introducing additional constraints or requiring higher order elements. This method is implemented in this paper using a novel linear 6DOF hexahedron element, where the three additional rotational degrees of freedom capture the asymmetry of shear strains in each respective plane. At the interface of two dissimilar materials, a coupling moment is measured in this degree of freedom which consequently enforces strain continuity across the interface; producing an asymmetric infinitesimal Cauchy stress tensor. In the case of a fibre-reinforced material under uniaxial tension, this coupling moment is necessary to physically model the constraint of rotations of the microstructural fibres in each ply toward the direction of an applied load due to the bonding of the two dissimilar materials. This additional micro-torsional energy captured in the model is reflected in the results produced, and is a mechanism that cannot be captured using classical continuum mechanics approaches.

A commonly used experiment for analysing free-edge effects is a symmetric, fixed width, four-ply laminate under uniaxial extension. Using classical methods, incompatibility of displacement gradient in adjacent plies give rise to large interlaminar stresses, with through-thickness normal stress exhibiting singular behaviour at the free-edge[2, 3]. Past attempts to address these non-physical stress predictions have included additional constraints or special treatment of the interface, or the use of higher-order elements[1, 5, 8]. Specialised solutions have been proposed which combine modified lamination theories to solve specific imposed boundary conditions[9]. The aim of this paper is to develop a generalised approach, which can address factors contributing to free-edge singularities in fibre-reinforced composite models, in order to predict failure mechanisms such as delamination.

The next section will outline the derivation of the orthotropic linear strain tensor and highlight its differences with classical continuum mechanics, before detailing its novel implementation into the finite element method. Following this, a numerical experiment involving a balanced angle-ply fibre-reinforced composite laminate under symmetric uniaxial loading will be used to assess the usability and physical significance of the IFT approach.

2 IMPLEMENTATION OF INTRINSIC FIELD TENSORS TO THE FINITE ELEMENT METHOD

2.1 The classical mechanical approach

The deformation gradient tensor $\mathbf{F}$ of a continuum can be expressed in tensor form as a function of the displacement gradient tensor $\nabla\mathbf{u}$ such that:

$$\mathbf{F} = \left(\nabla \mathbf{u} + \mathbf{I}\right)^{\mathrm{T}} \tag{1}$$

Here, ∇ refers to the forward gradient operator. On the scale of small deformations, the stretch $\mathbf{U}$ and rotation $\mathbf{R}$ tensors are defined as a result of an additive decomposition of the deformation gradient tensor into symmetric and skew-symmetric parts such that:

$$\mathbf{F} = \mathbf{U} + \mathbf{R} = \frac{1}{2}\left(\mathbf{F} + \mathbf{F}^{\mathrm{T}}\right) + \frac{1}{2}\left(\mathbf{F} - \mathbf{F}^{\mathrm{T}}\right) \tag{2}$$

It then follows that a linearized strain tensor $\boldsymbol{\varepsilon}$ can be approximated from the above definition of stretch; expressed in both tensorial and explicit component forms below

$$\boldsymbol{\varepsilon} \cong \mathbf{U} - \mathbf{I} = \frac{1}{2}\left[\nabla \mathbf{u} + \left(\nabla \mathbf{u}\right)^{\mathrm{T}}\right] \tag{3}$$

$$\varepsilon_{ij} = \frac{1}{2}\left(u_{i,j} + u_{j,i}\right) \tag{4}$$

The symmetrical nature of the infinitesimal strain tensor shown in Equation (4) is a result of the definition of a symmetric stretch $\mathbf{U}$ in the decomposition shown in Equation (2)

$$\therefore \varepsilon_{ij} = \varepsilon_{ji} \tag{5}$$

To distinguish with the novel strain tensor presented in the next section, Kellermann[7] denotes this symmetric linear strain tensor as the *Isotropic Linear Strain Tensor* (ILST); and its use hereon will be referred to as the classical continuum mechanics approach. The classical linearized rigid body rotation tensor $\boldsymbol{\omega}$ is defined as the skew-symmetric part of the displacement gradient tensor – written in component form below

$$\omega_{i\times j} = \frac{1}{2}\left(u_{j,i} - u_{i,j}\right) = \epsilon^{ijk}\omega_k \tag{6}$$

Here, ϵ^{ijk} are components of the third-order permutation tensor, used to define the positive sign convention of rotations on a given plane as a result of the cross product. It is important to note that in the classical continuum mechanics approach this rotation tensor is only a function of the geometric deformations of the body (the displacement gradient tensor). Note that we can express the following general definition relating strain and rigid body rotation as an additive decomposition of the displacement gradient

$$\nabla \mathbf{u} = \boldsymbol{\varepsilon} + \boldsymbol{\omega} \tag{7}$$

$$\therefore \varepsilon_{ij} = u_{j,i} - \epsilon^{ijk}\omega_k \tag{8}$$

The infinitesimal Cauchy stress tensor is obtained through a mapping of the ILST with the fourth-order material tensor $\mathbb{C}$, containing components C_{ijkl}, to form the constitutive equation:

$$\boldsymbol{\sigma} = \mathbb{C} : \boldsymbol{\varepsilon} \tag{9}$$

As a result of the symmetry of the ILST, in order to satisfy equilibrium of stresses on an element absent of applied body moments, classical mechanics requires only a single material constant (shear modulus) in order to entirely describe the shear response of a given plane. Therefore, in addition to major symmetry, the fourth-order material tensor $\mathbb{C}$ possesses the property that tensorial components describing behaviour on a particular shear plane are equal

$$C_{ijij} = C_{jiji} \tag{10}$$

For numerical calculations, in a three dimensional problem this condition allows for the amount of stress and strain components studied to be reduced from the full nine to the typically used reduced six.

2.2 The Intrinsic Field Tensor approach

The ILST derived in the classical continuum mechanics approach is based on an assumption of isotropic material behaviour; and therefore cannot correctly be automatically extended to the orthotropic case[7]. In other words, a linear strain tensor expressed only as a function of the geometric displacement response of a continuum is insufficient to describe the mechanical response of an orthotropic material due to its intrinsic directional material behaviour. The orthotropic-based elasticity theory is therefore primarily driven by the novel notion that that shear planes of an orthotropic media have distinct horizontal and vertical behaviour and thus in the constitutive law, a given plane requires two material constants to describe shear response

$$C_{ijij} \neq C_{jiji} \tag{11}$$

To now define an *Orthotropic Linear Strain Tensor* (OLST), we begin by decomposing the displacement gradient of a continuum into adapted linearized strain and rotation tensors; analogous to Equations (7) and (8)

$$\nabla \mathbf{u} = \boldsymbol{\text{æ}} + \boldsymbol{\varphi} \tag{12}$$

$$\therefore \text{æ}_{ij} = u_{j,i} - \epsilon^{ijk}\varphi_k \tag{13}$$

For the new elasticity theory, rather than the classical decomposition of the displacement gradient into simple symmetric and skew-symmetric parts, the novel OLST tensor is determined as a function of the orthotropic properties of the continuum. Hence, equilibrium is no longer solely enforced as a result of the geometric deformation of a continuum, but rather also dependent on the intrinsic material behaviour. We can define a set of general stress equilibrium equations on the continuum such that on a given plane

$$m_k = \epsilon^{ijk}\left(\sigma_{ji} - \sigma_{ij}\right) \tag{14}$$

Once more, components of the permutation tensor ϵ^{ijk} are used to denote the positive sign convention of the coupling moment m_k for each plane. In principle material directions, by using Equations (8) and (9), the above equation can then be expressed in terms of displacement gradient components and components of the fourth-order material tensor

$$m_k = \epsilon^{ijk}\left[C_{jiji}u_{i,j} - C_{ijij}u_{j,i} + \epsilon^{ijk}(C_{ijij} + C_{jiji})\varphi_k\right] \tag{15}$$

In a homogenous continuum, absent of any applied body moments, equilibrium states that all m_k must be zero. The material rotation tensor $\boldsymbol{\varphi}$ can then be explicitly determined – in terms of both displacement gradient components and material constants – where components are given by:

$$\epsilon^{ijk}\varphi_k = \frac{C_{ijij}u_{j,i} - C_{jiji}u_{i,j}}{C_{ijij} + C_{jiji}} \tag{16}$$

Unlike the classical form, which represented a geometric rigid body rotation, this new tensor gives a change in material principle direction[7]. From Equations (13) and (16), the closed form solution of the OLST is therefore also material property dependent, and is no longer assumed symmetric:

$$\text{æ}_{ij} = \frac{C_{jiji}}{C_{ijij} + C_{jiji}}\left(u_{i,j} + u_{j,i}\right) \tag{17}$$

$$\therefore \text{æ}_{ij} \neq \text{æ}_{ji} \tag{18}$$

By applying the classical isotropic material constraint on the constitutive law given in Equation (10) it becomes readily apparent this new definition reduces to form the ILST and corresponding infinitesimal rigid body rotation tensor $\boldsymbol{\omega}$ defined earlier – removing any dependence on the intrinsic material characteristics of the continuum:

$$\epsilon^{ijk}\varphi_k = \frac{1}{2}\left(u_{i,j} - u_{j,i}\right) = \epsilon^{ijk}\omega_k \tag{19}$$

$$\therefore \text{æ}_{ij} = u_{j,i} - \epsilon^{ijk}\varphi = \frac{1}{2}\left(u_{i,j} + u_{j,i}\right) = \varepsilon_{ij} \tag{20}$$

Significantly, the OLST shown here is an encompassing model which retains the ability to accurately model the isotropic case. This is opposed to the current approach of simply forcing the extension of the classical ILST derivation to the orthotropic case. The infinitesimal Cauchy stress tensor is formed as a result of the mapping of the OLST with a modified fourth-order constitutive law

$$\boldsymbol{\sigma} = \mathbb{C} : \boldsymbol{\text{æ}} \tag{21}$$

In the orthotropic case, due to the asymmetric nature of the strain tensor, numerical methods must explicitly determine all nine distinct components of stress and strain on a three-dimensional element. It will be shown in the numerical experiment to follow that at the interface between two dissimilar orthotropic materials in a continuum, the new method allows for an asymmetric Cauchy stress tensor, which has significant physical meaning in the analysis of fibre-reinforced composites.

2.3 Application to Finite Element Method:

The new orthotropic-based elasticity theory presented in Section 2.2 can be incorporated into simple linear 2D and 3D elements simply through manipulating the calculation of the typical stiffness matrix relating forces and displacements. In this paper, an 8-noded isoparametric linear hexahedral element will be considered. In order to implement the classic ILST into the finite element method, we are required to capture only 3DOF per node (3 translational displacements). Therefore the classical element can be attributed the following displacement vector

$$q_{\text{ILST}} = \left[u_1,\ u_2,\ u_3\right]^{\text{T}} \tag{22}$$

Here, element displacements u_i are a linear interpolation of the respective displacements from each node i, (where N_i are linear shape functions)

$$u_1 = \sum_{i=1}^{8} N_i u_{1(i)} \qquad u_2 = \sum_{i=1}^{8} N_i u_{2(i)} \qquad u_3 = \sum_{i=1}^{8} N_i u_{3(i)} \tag{23}$$

However, each node of the proposed orthotropic hexahedral element is capable of capturing 6DOF (3 translational displacements, 3 rotations). For the new orthotropic-based element, we therefore attribute the following extended displacement vector:

$$q = \left[u_1,\ u_2,\ u_3,\ \varphi_1,\ \varphi_2,\ \varphi_3\right]^{\text{T}} \tag{24}$$

Once more, components of the above displacement vector are determined as a linear interpolation of the value at each node using similar expressions for the rotational degrees of freedom to those shown in Equation (23)

$$\varphi_1 = \sum_{i=1}^{8} N_i \varphi_{1(i)} \qquad \varphi_2 = \sum_{i=1}^{8} N_i \varphi_{2(i)} \qquad \varphi_3 = \sum_{i=1}^{8} N_i \varphi_{3(i)} \tag{25}$$

The asymmetry of the OLST requires all 9 distinct components of strain and stress to be determined. In principle directions, these second-order tensors can be flattened to vector form using Voigt notation, such that

$$\boldsymbol{\sigma}^{\{M\}} = [\sigma_{11}, \sigma_{22}, \sigma_{33}, \sigma_{23}, \sigma_{31}, \sigma_{12}, \sigma_{32}, \sigma_{13}, \sigma_{21}]^{\text{T}} \tag{26}$$

$$\boldsymbol{\varpi}^{\{M\}} = [\varpi_{11}, \varpi_{22}, \varpi_{33}, \varpi_{23}, \varpi_{31}, \varpi_{12}, \varpi_{32}, \varpi_{13}, \varpi_{21}]^{\text{T}} \tag{27}$$

Here, $\{M\}$ denotes the principle material coordinate system. From the orthotropic-based constitutive law presented in Equation (21) the fourth order material tensor $\mathbb{C}$ can be flattened to matrix form such that

$$\boldsymbol{\sigma}^{\{M\}} = \mathbf{C}^{\{M\}} . \boldsymbol{\varpi}^{\{M\}} \tag{28}$$

Here, $\mathbf{C}^{\{M\}}$ is the material matrix for a given element in principle material directions. This matrix is symmetric, invertible and of size $[9 \times 9]$. The material matrix can be transformed to the global coordinate system $\{G\}$ through an angle θ using the orthogonal rotation matrix $\mathbf{T}$ such that

$$\mathbf{C}^{\{G\}} = \mathbf{T}^{-1}(\theta) . \mathbf{C}^{\{M\}} . \mathbf{T}(\theta) \tag{29}$$

For a transversely isotropic fibre-reinforced material, θ is typically used to describe the angle of which fibres are offset from the global Cartesian longitudinal axis. As discussed in Section 2.2, in the new approach equilibrium is to be determined as a result of the distinct shear behaviour in different directions on a given plane. Hence, the equilibrium equations given in Equation (15) are resolved as

part of the finite element process – rather than through an applied symmetry constraint to the system. To achieve this, the strain vector in Equation (27) is written in terms of the decomposition of the displacement gradient tensor shown in Equation (13) where rotation tensor components are resolved as variables in the model, captured through the additional degrees of freedom

$$\bar{\text{œ}}^{\{M\}} = \left[u_{1,1},\ u_{2,2},\ u_{3,3},\ u_{3,2},\ u_{1,3},\ u_{2,1},\ u_{2,3},\ u_{3,1},\ u_{1,2},\ \varphi_1,\ \varphi_2,\ \varphi_3 \right]^{\mathrm{T}} \tag{30}$$

Similarly, we introduce the equilibrium equations given in Equation (14) to the constitutive law by extending the stress vector shown in Equation (26)

$$\bar{\sigma}^{\{M\}} = [\sigma_{11},\ \sigma_{22},\ \sigma_{33},\ \sigma_{23},\ \sigma_{31},\ \sigma_{12},\ \sigma_{32},\ \sigma_{13},\ \sigma_{21},\ m_1,\ m_2,\ m_3]^{\mathrm{T}} \tag{31}$$

Simple manipulation of the constitutive law in principle directions to extend the linear system of equations results in a modified $[12\times12]$ matrix $\bar{\mathrm{C}}^{\{M\}}$; which importantly remains symmetric and invertible, and can be transformed to global coordinates using an extended rotation tensor $\bar{\mathrm{T}}(\theta)$, analogous to Equation (29):

$$\bar{\mathrm{C}}^{\{G\}} = \bar{\mathrm{T}}^{-1}(\theta).\bar{\mathrm{C}}^{\{M\}}.\bar{\mathrm{T}}(\theta) \tag{32}$$

At a given node, the displacement gradient components forming extended strain vector $\bar{\text{œ}}^{\{M\}}$ are approximated using a matrix of differentials such that

$$\bar{\text{œ}}^{\{G\}} = [\partial].q \tag{33}$$

The components of the differential matrix, are numerically calculated by introducing the interpolation expressions (23) and (25) to extend the vector q, and rearranging terms to form a matrix B such that

$$\bar{\text{œ}}^{\{G\}} = \mathrm{B}.Q \tag{34}$$

Here, Q is a vector containing all displacements at each node (i) in an element

$$Q = \left[u_{1(1)},\ u_{2(1)},\ u_{3(1)},\ \varphi_{1(1)},\ \varphi_{2(1)},\ \varphi_{3(1)},\ \dots,\ u_{1(8)},\ u_{2(8)},\ u_{3(8)},\ \varphi_{1(8)},\ \varphi_{2(8)},\ \varphi_{3(8)} \right]^{\mathrm{T}} \tag{35}$$

The contents of matrix B are determined through differentiation of the linear isoparametric shape functions, and converting between natural and global coordinate systems using the Jacobian matrix J:

$$\mathrm{J} = \begin{bmatrix} \frac{\partial x}{\partial \xi} & \frac{\partial y}{\partial \xi} & \frac{\partial z}{\partial \xi} \\ \frac{\partial x}{\partial \eta} & \frac{\partial y}{\partial \eta} & \frac{\partial z}{\partial \eta} \\ \frac{\partial x}{\partial \mu} & \frac{\partial y}{\partial \mu} & \frac{\partial z}{\partial \mu} \end{bmatrix} = \sum_{i=1}^{8} \begin{bmatrix} x_i \frac{\partial N_i}{\partial \xi} & y_i \frac{\partial N_i}{\partial \xi} & z_i \frac{\partial N_i}{\partial \xi} \\ x_i \frac{\partial N_i}{\partial \eta} & y_i \frac{\partial N_i}{\partial \eta} & z_i \frac{\partial N_i}{\partial \eta} \\ x_i \frac{\partial N_i}{\partial \mu} & y_i \frac{\partial N_i}{\partial \mu} & z_i \frac{\partial N_i}{\partial \mu} \end{bmatrix} \tag{36}$$

Through Gaussian integration, the stiffness matrix for the element (e) is given by

$$\mathrm{K}^{(e)} = \int_{V^{(e)}} \mathrm{B}^{\mathrm{T}} \bar{\mathrm{C}}^{\{G\}} \mathrm{B} \; dV^{(e)} = \sum_{i=1}^{p_1} \sum_{j=1}^{p_2} \sum_{k=1}^{p_3} w_i w_j w_k \; . \mathrm{B}_{ijk}{}^{\mathrm{T}} \; . \bar{\mathrm{C}}^{\{G\}} \; . \mathrm{B}_{ijk} \det \mathrm{J} \tag{37}$$

Here, w_i and p_i are the Gaussian weights and integration points respectively, and $dV^{(e)}$ is the volume of the infinitesimal element

Note that using this new 6DOF linear finite element and applying the classical constraint stating that the two material constants defining shear in a given plane are equal will produce identical results to the linear 3DOF hexahedral element described at the beginning of this section.

3 CASE STUDY: FREE-EDGE STRESSES IN COMPOSITE LAMINATES

3.1 Details of Numerical Experiment

Figure 1 shows a symmetric angle-ply laminate of fibre-reinforced material (T700/VTM264) [10] under uniaxial extension along the longitudinal axis. The laminate has a width of $b =$ 18 mm and has four plies each of thickness $h =$ 1 mm. The principle orientation of the fibres in a given layer is offset from the longitudinal axis by an angle θ. The lay-up sequence of the composite laminate studied in this paper is a balanced angle-ply of the form: $[-\theta / +\theta]_s$

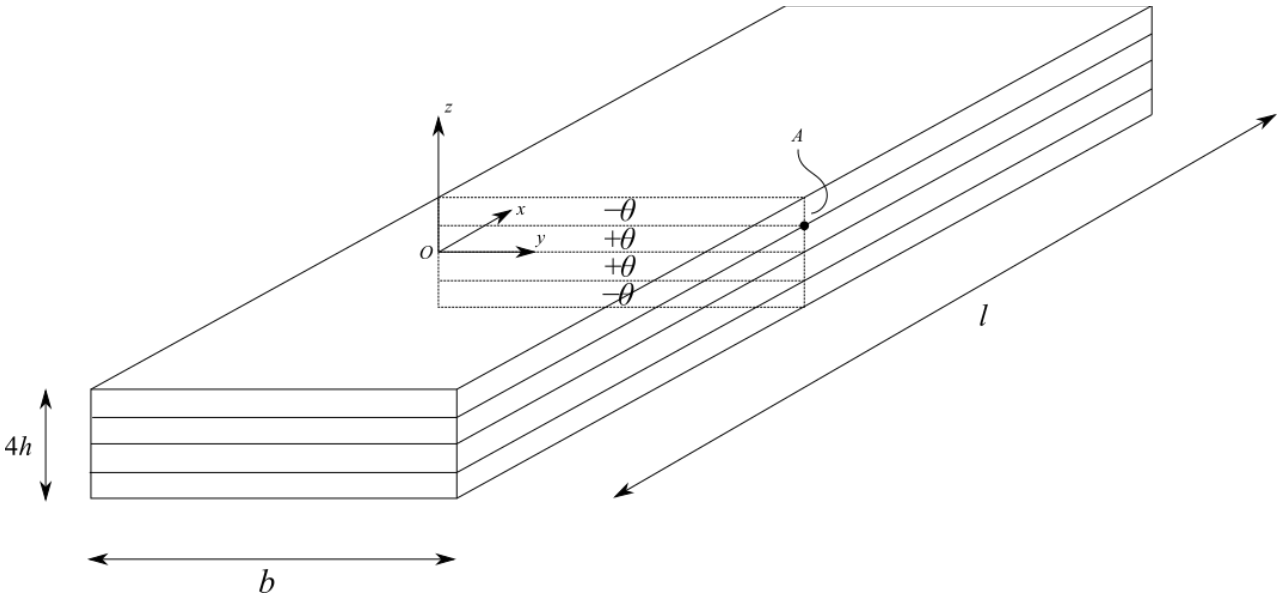

Figure 1 - Details of Numerical Experiment

In the finite element model, using displacement control, the coupon is extended such that an arbitrarily chosen constant axial strain is imposed ($\varepsilon_{xx} = 0.0001$). We are interested in the interlaminar stress response between dissimilar layers, particularly along the transverse axis y as we approach the interface corner (marked point A in Figure 1). At the free-edge, classical methods predict singularities in the zz and zx components of the stress tensor[2]. The composite is constructed of four layers of fibre-reinforced composite, each ply idealised as homogenous and elastic using the material properties (in primary material coordinates) provided in Table 1

Material Property		T700/VTM264
E_1	[MPa]	120200
E_2, E_3	[MPa]	7467
G_{12}, G_{13}	[MPa]	3904
G_{23}	[MPa]	2304
ν_{12}, ν_{13}	–	0.32
ν_{23}	–	0.33

Table 1 - Material properties of fibre-reinforced composite used in numerical experiment[10]

In order to assess any singular behaviour in stress components, the balanced angle-ply laminate has been discretised using four meshes of increasing refinement, with more elements favoured towards the free-edge of the specimen in each case: Coarse, Medium, Fine and Very Fine (800, 6400, 51200 and 172800 elements respectively)

3.2 Discussion of Results

Figure 2 shows the calculated transverse shear stress at the point *A* indicated in Figure 1 for symmetric $[-\theta/+\theta]_s$ angle-ply laminates ranging from $\theta = 0°$ to $90°$. For this shear component, the peak value occurs at the free-edge, whilst the component vanishes towards the centre of the specimen. Singular behaviour in the stress component can be observed for both the classical and IFT approaches, with the new model predicting slightly lower values. The classical approach shows good agreement with results presented by both Becker[11] and Herakovich[12], whereby the maximal interlaminar shear occurs for the lay-up angle $\theta = 15°$. This therefore provides a solid basis to assess the IFT approach.

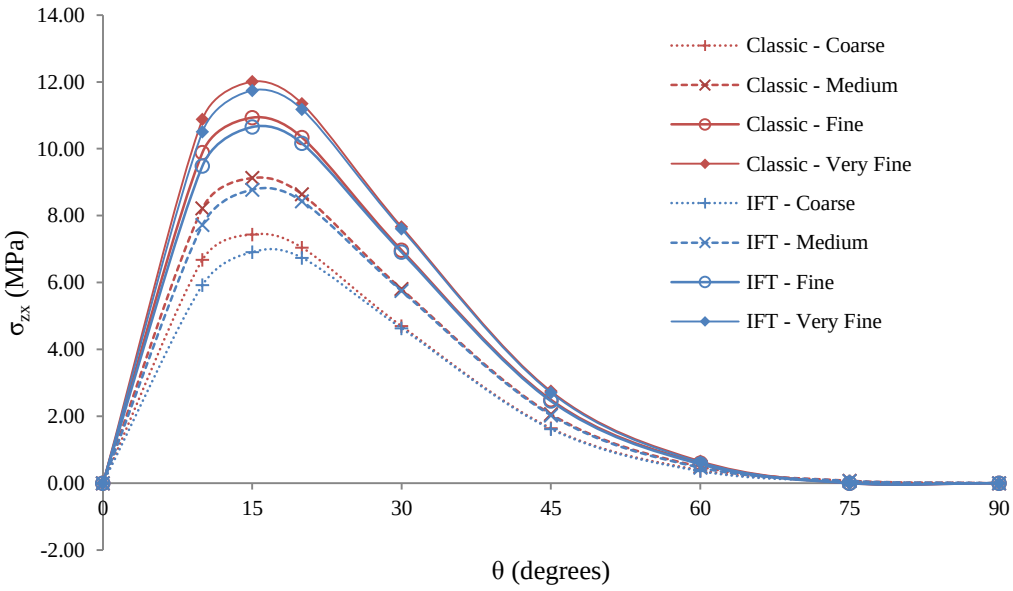

Figure 2 – Free-edge interlaminar shear stress σ_{zz} for a range of $[-\theta/+\theta]_s$ laminates

The behaviour of the through-thickness normal stress component along the interface plane consists of a steep stress gradient approaching the free-edge, with the maximum value occurring at Point *A* (Figure 1). These maximal values are shown below in Figure 3 for the same range of lay-up angles.

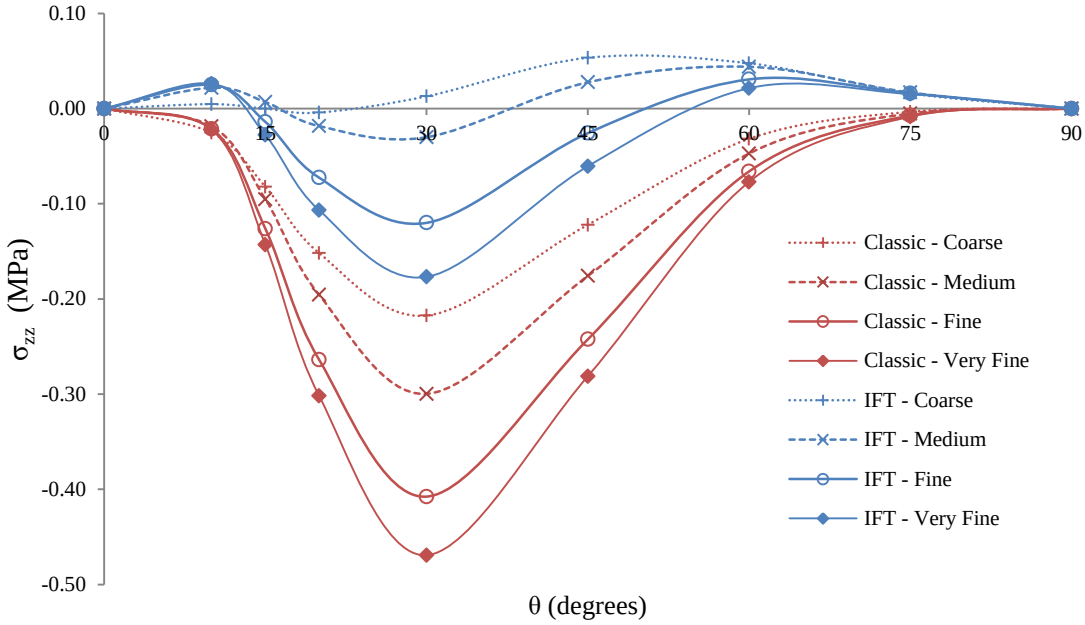

Figure 3 – Free-edge through-thickness normal stress σ_{zz} for a range of $[-\theta/+\theta]_s$ laminates

Using the symmetry-based ILST, classical mechanics predicts a compressive singularity for all lay-up angles θ. A maximum occurs at a lay-up angle close to $30°$, and these results replicate predictions offered in the literature [2, 3, 8]. The novel IFT finite element predicts significantly lower stresses and the singular behaviour is reduced for all lay-up angles. The orthotropic-based approach predicts converging tensile behaviour for $\theta < 15°$ and $\theta > 50°$, whilst the mid-range predicts a compressive singularity.

Free-edge singularities are a well-researched topic in continuum mechanics. These non-physical predictions can be said to be multi-modal, with several factors contributing to their development at the interface of dissimilar materials. Among others, these include the intersection of distinct isotropic elastic properties[13], the effect of different Poisson's ratios in adjacent plies, and the bonding of anisotropic materials with opposing principle material directions. It has been shown, that by addressing the latter of these, for balanced angle-ply laminates under symmetric uniaxial tension, the approach presented in this paper has had minimal effect on transverse shear stresses, though greatly reduced the free-edge singularity found in the σ_{zz} component. In future studies it would be desirable to isolate the extent of which certain other factors contribute to this singularity in order to completely assess the significance of this work.

Accurate predictions of the through-thickness normal strain component are requisite in understanding the failure mechanisms of composite laminates. It is known that there are three distinct failure modes in composites, with smaller angle lay-ups failing in delamination and the larger angle plies undergoing lamina failure[14]. For the preliminary results of the IFT finite element approach shown in Figure 3, the three distinct ranges of stress behaviour outlined earlier tend to occur in ranges that match those different failure mechanisms. This is more useful than classical mechanics which

predicts a compressive singularity for all laminates, regardless of their known different methods of failure.

As outlined in the derivation, a significant property of the new model is its encompassment of isotropic behaviour. For a homogenous material, the novel orthotropic finite element will reduce to calculate stress results matching those of classical mechanics. This can be observed in the results of the $0°$ and $90°$ lay-up angles in both Figures 2 and 3. The IFT model provides an improved physical understanding of the deformation mechanisms occurring in a fibre-reinforced laminate under tension.

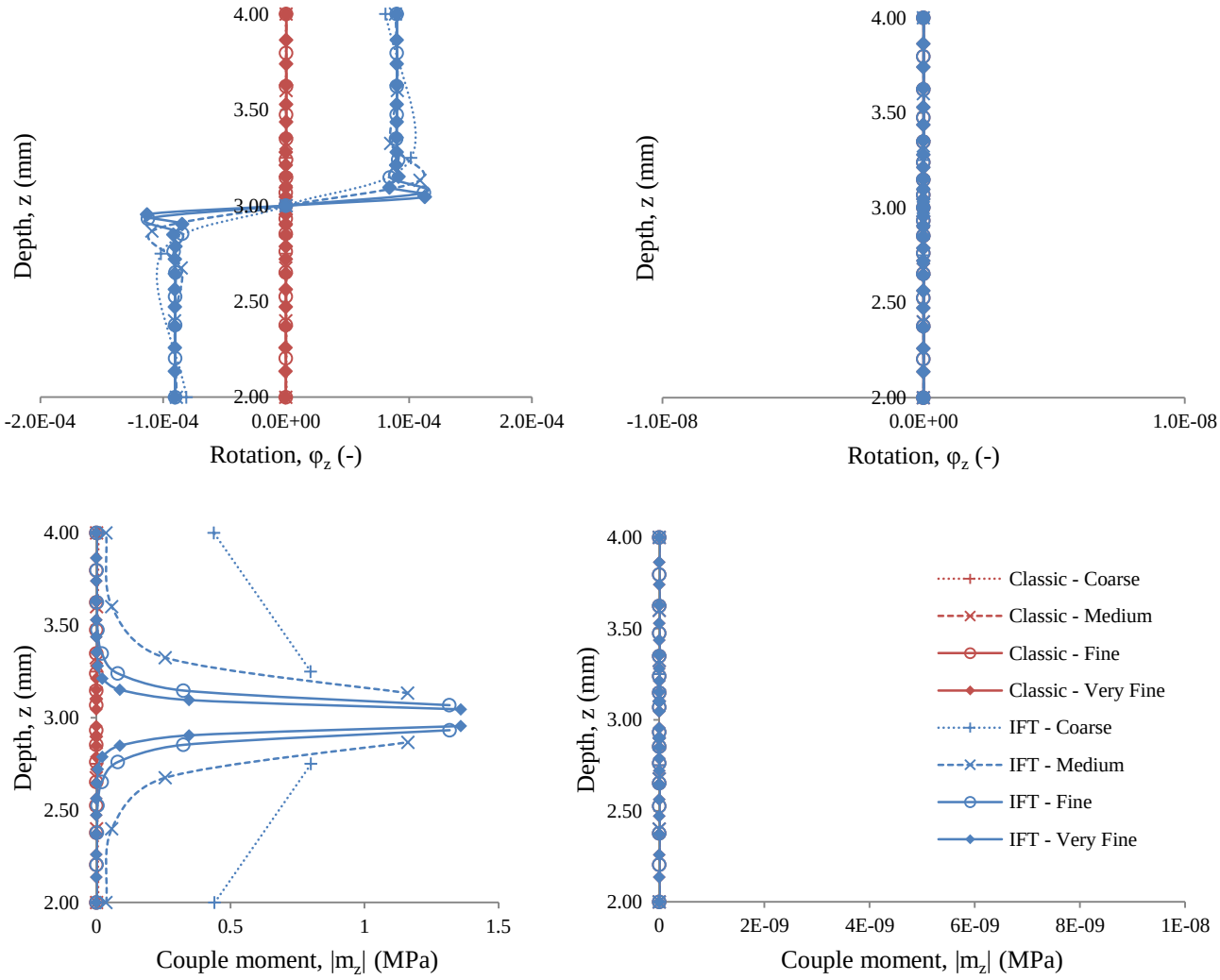

Figure 4 - In-plane rotations (top) and couple moments (bottom) versus laminate depth for $[-30°/+30°]_s$ and $[-0°/+0°]_s$ laminates (left and right respectively)

The in-plane material rotation around the z axis, as defined in Equation (13), is shown in the top row of Figure 4. Recall that this is a measure of the asymmetry of strain in a given plane. For a lay-up angle $0°$, as expected we observe the new formulation reduces to match the classical response. For the $30°$ case, we observe that the new formulation indicates that the $+30°$ and $-30°$ layers rotate relative to each other as fibres attempt to align in the direction of the applied load. As the material is assumed perfectly bonded, the rotation at the interface correctly is zero, and strain continuity is ensured. To enforce this, a couple moment, defined in Equation (14), is captured at the interface which physically

represents the resistance to load caused by bonding two anisotropic materials with opposing principle fibre directions. Similar results are observed for all other lay-up angles θ. Classical mechanics is unable to capture this additional torsional energy; instead adding it to the high stress gradient at the free-edge. This explains the reduction in singular behaviour we observe in Figure 3 by using the new orthotropic-based theory to addresses this issue.

4 CONCLUSIONS

A novel linear 3D finite element is derived in this paper which removes a symmetry assumption inherent in classical mechanics through implementation of an orthotropic-based elasticity theory dependent on the intrinsic material properties of the system. This new approach is a generalised model which can be applied to any geometry or loading conditions without the requirement for special treatment of interfaces or lamination theories. The model is shown to have physical significance in both its theories and application. Numerical investigation of a transversely isotropic balanced angle-ply composite laminate shows a reduction in the singularity as a result of capturing the additional torsional energy resulting from the bonding of adjacent layers with distinct anisotropic principle material directions. When symmetric isotropic shear material behaviour is reintroduced, the model collapses to classical continuum mechanics theory, and equivalent results to past literature are replicated. Future experimental work is needed to consolidate these preliminary findings, and detect the suitability of the new approach in predicting failure mechanisms of fibre-reinforced composites.

REFERENCES

[1] Kim, H.S., J. Lee, and M. Cho, *Free-edge interlaminar stress analysis of composite laminates using interface modeling.* Journal of Engineering Mechanics, 2011.

[2] Pagano, N., *Free edge stress fields in composite laminates.* Mechanics of Composite Materials, 1994: p. 304-311.

[3] Schellekens, J. and R. De Borst, *Free edge delamination in carbon-epoxy laminates: a novel numerical/experimental approach.* Composite structures, 1994. **28**(4): p. 357-373.

[4] Salamon, N.J., *An assessment of the interlaminar stress problem in laminated composites.* Journal of composite materials, 1980. **14**(1): p. 177-194.

[5] Schellekens, J. and R. De Borst, *A non-linear finite element approach for the analysis of mode-I free edge delamination in composites.* International Journal of Solids and Structures, 1993. **30**(9): p. 1239-1253.

[6] Cosserat, E. and F. Cosserat, *Theory of Deformable Bodies, Scientific Library, A.* Hermann and Sons, Paris, 1909.

[7] Kellermann, D., T. Furukawa, and D. Kelly, *Strongly orthotropic continuum mechanics and finite element treatment.* International journal for numerical methods in engineering, 2008. **76**(12): p. 1840-1868.

[8] Raju, I. and J.H. Crews Jr, *Interlaminar stress singularities at a straight free edge in composite laminates.* Computers & Structures, 1981. **14**(1): p. 21-28.

[9] Pipes, R.B. and N. Pagano, *Interlaminar stresses in composite laminates under uniform axial extension*, in *Mechanics of Composite Materials*. 1994, Springer. p. 234-245.

[10] Ahamed, J., et al., *Ply-interleaving technique for joining hybrid carbon/glass fibre composite materials.* Composites Part A: Applied Science and Manufacturing, 2016. **84**: p. 134-146.

[11] Becker, W., *Free-edge stress concentration in angle-ply laminates.* Archive of Applied Mechanics, 1994. **65**(1): p. 38-43.

[12] Herakovich, C., *Free edge effects in laminated composites.* 1989.

[13] Whitcomb, J., I. Raju, and J. Goree, *Reliability of the finite element method for calculating free edge stresses in composite laminates.* Computers & Structures, 1982. **15**(1): p. 23-37.

[14] Rotem, A. and Z. Hashin, *Failure modes of angle ply laminates.* Journal of Composite Materials, 1975. **9**(2): p. 191-206.